Ocean Engineering 153 (2018) 215–224

Contents lists available at ScienceDirect

Ocean Engineering

journal homepage: www.elsevier.com/locate/oceaneng

Ship voyage optimization for safe and energy-efficient navigation: A dynamic programming approach

R. Zaccone [a,*], E. Ottaviani [b], M. Figari [a], M. Altosole [a]

[a] DITEN - Department of Electrical, Electronic, Telecommunications Engineering and Naval Architecture, Polytechnic School, University of Genoa, Genoa, Italy
[b] OnAIR s.r.l., Genoa, Italy

ARTICLE INFO

Keywords:
Ship voyage optimization
Dynamic programming
Weather routing
Ship propulsion
Ship motions

ABSTRACT

The paper presents a 3D dynamic programming based ship voyage optimization method, aiming to select the optimal path and speed profile for a ship voyage on the basis of weather forecast maps. The optimization is performed in accordance to a minimum fuel consumption strategy taking also into account ship motions and comfort. The optimization is carried out in a discretized space-time domain: the ship voyage is parametrized as a multi-stage decision process in order to formulate a dynamic programming optimization problem. Waves and wind conditions are estimated for each route segment by weather forecasting maps then seakeeping related indexes and fuel oil consumption are computed taking into account wave-induced ship motions and added resistance. The best routing solution is thus selected by a dynamic programming algorithm developed and implemented by the authors. Results and discussion of the proposed method are presented for a merchant ship application in a test case voyage through the Northern Atlantic Ocean and compared to the constant speed great circle solution.

1. Introduction

In the recent years the continuously increasing availability of reliable weather forecast data has significantly improved the safety of the ship voyages, helping the operators to select proper routes to avoid rough weather and have an estimate of the time of arrival (ETA) and the voyage cost. Moreover, increased attention is put nowadays to seakeeping abilities of ships in order to improve passage safety even with rough sea. However, most of the time medium intensity weather conditions are encountered; these conditions do not affect ship safety but influence fuel consumption and comfort on board. In this framework optimization algorithms can provide a significant support to the decision making process in order to select the best choice in sight of one or more objectives.

The selection of the optimal route combines a number of objective functions as well as various constraints. In principle a ship voyage is characterized by a starting point, an arrival point, a constrained arrival time window, eventually a number of fixed way points. Geographical (static) constraints need to be considered as well: for example, the shore line, traffic separation schemes, restricted areas, bathymetry. Realistic modeling of the ship behaviour in relation to weather conditions is crucial to correctly estimate and compare the ship performance in different conditions. Decision making needs to be based on ship response, rather than on external conditions (Chen, 2013), in order to better fit different ship types, shapes and dimensions: different ships have different responses in the same weather and speed conditions. Ship and human life safety, fuel consumption, energy efficiency, crew and passengers comfort, voyage time management, control of delays are possible tasks which can be pursued by voyage optimization.

Weather routing services and codes available on the market are usually not supported by public domain scientific papers due to confidentiality reasons. In author's knowledge very often they are based on the principle of 'storm avoidance'. The typical approach is to implement a set of generic speed reduction curves in function of sea state parameters (for example the Beaufort Wind Force Scale) and a number of global ship parameters (for example, displacement and length). The fuel consumption is estimated on the basis of empirical relationships, while ship hull geometry, seakeeping abilities and propulsion system features are neglected. This approach can lead to unnecessary diversions to avoid rough weather, badly affecting the fuel consumption. The ship speed decrease in rough weather can occur as a consequence of two reasons: involuntary speed reduction due to the additional resistance induced by wind and waves, and/or voluntary speed reduction to avoid navigation hazards and excessive ship motions which would result in propeller racing, slamming or green water. Additional constraints related to safety

* Corresponding author.
E-mail address: raphael.zaccone@edu.unige.it (R. Zaccone).

https://doi.org/10.1016/j.oceaneng.2018.01.100
Received 16 March 2017; Received in revised form 19 October 2017; Accepted 25 January 2018
Available online 4 February 2018

and/or comfort might thus be considered to limit ship motions or wave induced forces. A proper ship response modeling is crucial in order to correctly estimate these phenomena on a case by case basis. Furthermore a model of the actual propulsion system is essential in order to predict the propulsion performances in rough sea and to take into account the propulsion system limits when steaming into stormy conditions. Moreover, ship speed changes need to be managed by the optimization algorithm in order to use the speed adjustment as a rough weather avoidance parameter in addition to course deviation but within the propulsion system thrust/power capability.

The weather routing problem has been addressed by many authors in the past and different approaches have been proposed. The first pioneer works were centred on finding the minimum time of arrival on a voyage (James, 1957; Zoppoli, 1972; Papadakis and Perakis, 1990) however most of the authors neglected the ship response behaviour in rough sea. More recently, voyage optimization has been approached in a wider sense, taking into account ship motions and/or fuel consumption. The most used techniques include multi objective genetic algorithms (Marie et al., 2009; Maki et al., 2011; Vettor and Guedes Soares, 2016; Zaccone et al., 2016), deterministic enumerative algorithms (Lin et al., 2013; Fang and Lin, 2015; Shao et al., 2012), brute force optimization (Lu et al., 2015), local search algorithms (Safaei et al., 2015). Simulation of ship behaviour in rough sea have been proposed in the past by several authors: Journée (1976); Journée and Meijers (1980) proposed some guidelines to develop a ship model to take into account either propulsion and ship motions. More recently weather routing oriented propulsion simulation, without optimization, have been published by Coraddu et al. (2013). Crew and passengers comfort evaluation techniques for human bodies exposed to mechanical vibrations and accelerations are suggested in the ISO 2631-1: 1997, based on the methods proposed by O'Hanlon and McCauley (1973), and Lawther and Griffin (1988). The authors gained extensive experience in steady state and transient modeling of ship propulsion systems (Altosole et al., 2008, 2014, 2016, 2017; Martelli et al., 2014a,b) mainly for control design purposes.

In the here presented work ship voyage optimization problem is tackled by means of a problem-specific algorithm based on 3D dynamic programming (3DDP) coupled with a dynamic ship propulsion model and with weather forecast data. Fuel oil consumption is considered as the objective function to minimize while ship motions and expected time of arrival (ETA) are used as constraints. In particular, ship motions based constraints are imposed on probability of slamming and deck wetness (Journée and Meijers, 1980), motions sickness index (MSI) (O'Hanlon and McCauley, 1973), and lateral forces (Perez, 2006). The constraints allow to implicitly take into account any voluntary speed reduction in presence of rough weather, while involuntary speed reductions are simulated by considering the effect of the ship resistance increase due to waves (Journée, 1976) on the propulsion system. Wave and wind forecast data are considered in function of time and geographical coordinates: wave significant height, mean period, direction and wind speed components are obtained via space-time interpolation in the forecast maps. The obtained data are used to estimate ship motions and added resistance in order to assess the required engine power and fuel consumption via steady state ship propulsion simulation. The fuel consumption is used as the cost function to evaluate each route segment and compute the optimal solution. DP approach fits well to 'best path search' problems (Bellman, 1958), so is one of the classic choices to tackle ship voyage optimization tasks. In particular, the problem is solved by exhaustively exploring a discretization of the search domain while very little restrictions are put on either the objective function and optimization constraints because no derivatives are calculated. The deterministic nature of the algorithm may be seen as an advantage with respect to heuristic global search algorithms. Nevertheless, in a weather routing framework, the benefit is partially limited by the fact that input data is affected by significant uncertainties. DP method has some drawbacks in terms of compuatation speed. However, the presented implementation includes proper problem-specific pruning strategies to boost computational efficiency. The implemented algorithm performs an efficient systematic exploration of the domain of the solutions, defined by a three dimensional space time grid. The result of the optimization is a sequence of waypoints and intermediate times determining the ship trajectory and speed profile. With respect to present state of the art weather routing and voyage optimization methods, the presented approach presents a twofold benefit: it is based on a detailed description of the propulsion system allowing a realistic evaluation of the fuel consumption and exhaust emissions versus ship speed and it implements an innovative 3D dynamic programming optimization routine which allows to manage both ship route and speed profile.

To this end, the main tasks to be solved, in order to manage the route optimization problem, are:

- weather forecast data availability and management;
- ship propulsion performance and hydrodynamic response modeling;
- optimization problem formulation and solution.

A short overview is given to the first point, which is considered as input data. The paper is centred on the second and third points which are going to be described in detail. Finally, a case study is analysed and results are shown in order to highlight the features of the presented approach in a realistic case.

2. Weather conditions

Two weather actions are considered: waves and wind. Wind forecast data is provided in terms of wind speed components (u, v) as a function of geographical coordinates (λ, φ) and time t. Forecasted wave significant parameters are provided as well in function of the same variables, in particular significant wave height $H_{\frac{1}{3}}$, wave period T_1, and direction θ. The wave parameters are used to fit a parametric spectral formulation. ITTC 84 JONSWAP spectral formulation with a cosine square spreading function is used:

$$S(\omega,\theta) = 155\frac{H_{\frac{1}{3}}^2}{\omega^5 T_1^4}\exp\left(-\frac{944}{\omega^4 T_1^4}\right)\gamma^Y\frac{2}{\pi}\cos^2\theta \tag{1}$$

being:

$$Y = \exp\left[-\left(\frac{0.191\omega T_1 - 1}{\sqrt{2}\sigma}\right)\right] \tag{2}$$

where ω is the wave circular frequency, and $\gamma = 3.3$ for Northern Atlantic applications. The choice of the spectral formulation can significantly affect the results, as it directly influences the ship motions and resistance. In particular, a correct selection of parameter γ should be made in function of the geographical area in which the optimization is performed. Moreover, real and parametric spectra may differ significantly in presence of crossing seas (Mentaschi et al., 2015; Spentza et al., 2017): these aspects will be deeply investigated in the future research, while the presented work is mainly focused on investigating the potential of the optimization procedures in a voyage optimization framework.

3. Ship model

The ship numerical model allows to estimate the fuel consumption in given geographical positions, weather conditions and ship speeds. The model is structured in four main blocks:

- hydrodynamic resistance calculation
- ship motions and comfort assessment
- propeller performance prediction
- engine performance prediction

The model arrangement is shown in Fig. 1. At any time and

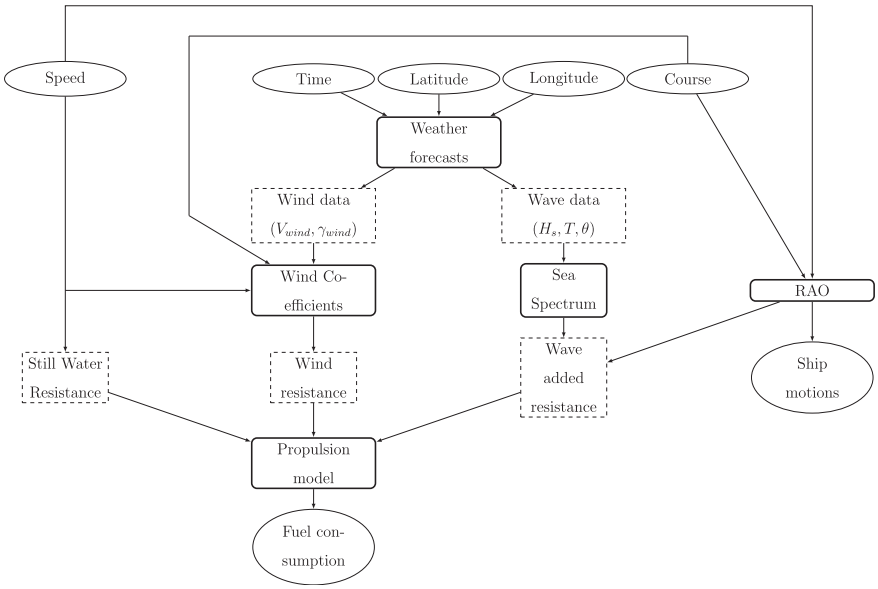

Fig. 1. A scheme of the ship model arrangement.

geographical coordinates the weather conditions (wave and wind data) are estimated by interpolating into weather forecast data then the hydrodynamic resistance as well as ship motions are computed. Finally the required propeller thrust and torque are evaluated using propeller open water diagrams in order to finally assess the engine power and fuel consumption.

3.1. Resistance

The hydrodynamic resistance of the ship, R_{tot}, is decomposed in accordance with the following equation:

$$R_{tot} = R_t + R_{aw} + R_{wind} \tag{3}$$

where R_t is the still water hydrodynamic resistance, R_{aw} is the added resistance due to the rough sea effect, and R_{wind} is the wind resistance. The added wave resistance R_{aw} is estimated according to the following expression (Lewis, 1989):

$$R_{aw} = \int_0^{\infty}\int_0^{2\pi} \Phi_{aw} S_{\zeta} d\omega d\mu \tag{4}$$

where ω is the wave circular frequency, S_{ζ} is the directional wave energy spectral density, $\Phi_{aw}(\omega, \theta, V)$ is the wave added resistance pseudo-response amplitude operator (which expresses the longitudinal drift forces per squared wave amplitude and wave circular frequency) and μ is the encounter angle.

The wind resistance R_{wind} is expressed through a function of the relative wind speed $V_{w,r}$:

$$R_{wind} = \frac{1}{2}\rho_{air} A_F V_{w,r}^2 c_X(\gamma_w) \tag{5}$$

where ρ_{air} is the air density, A_F is the ship's above water front projection area and c_X is the wind resistance coefficient depending on the encounter angle γ_w. The effects of rough weather are thus modelled in terms of resistance increase rather than speed reductions: the resistance increase is actually the cause of the involuntary speed reduction or the power output increase to achieve the required speed (within engine limits).

3.2. Ship motions and comfort

The energy spectrum of absolute motion η_i is evaluated in accordance with the following equation (Lewis, 1989):

$$S_{\eta_i} = \left|RAO_{\eta_i}\right|^2 S_{\zeta} \tag{6}$$

where ω is the wave circular frequency, μ is the encounter angle, $S_{\zeta}(\omega, \mu)$ is the directional wave energy spectral density, and RAO_{η_i} is the complex response amplitude operator of motion η_i, with $i = 1$ to 6 represent surge, sway, heave, roll, pitch and yaw motions respectively. The probability that motion η_i exceeds the value η_i^* is given by the following relationship:

$$P\left(\eta_i > \eta_i^*\right) = \exp\left[-\frac{\left(\eta_i^*\right)^2}{2m_{0\eta_i}}\right] \tag{7}$$

where $m_{0\eta_i}$ is the spectral moment of order zero of motion η_i. The joint probability that motions η_i and η_j exceed the values η_i^* and η_j^* respectively, is obtained under the hypothesis of independence between η_i and η_j, and is given by the following formula:

$$P\left(\eta_i > \eta_i^*, \eta_j > \eta_j^*\right) = \exp\left\{-\left[\frac{\left(\eta_i^*\right)^2}{2m_{0\eta_i}} + \frac{\left(\eta_j^*\right)^2}{2m_{0\eta_j}}\right]\right\} \tag{8}$$

The spectral moment of order n per squared wave height of motion η_i is given by:

$$m_{n,1} = \int_0^{\infty}\int_0^{2\pi} \omega^n S_{\eta_i} d\omega d\mu \tag{9}$$

Lateral force estimator (LFE) is used as a global index to take into account either lateral accelerations and displacements (Perez, 2006). The LFE at the point P of cartesian coordinates (x_P, y_P, z_P) is given by the following equation:

$$LFE_P = \ddot{\eta}_2 - \ddot{\eta}_4\left(z_P - z_g\right) + \ddot{\eta}_6\left(x_P - x_g\right) - g\eta_4 \tag{10}$$

where $\ddot{\eta}_i$ represent the acceleration of motion η_i. The above mentioned equation is an expression of side component of the apparent acceleration acting on a body on a ship, expressed in its relative system of coordinates, simplified for small amplitude motions. In particular, The first term represents the acceleration induced by the sway motion, the second and third express the contributes due to roll and yaw angular accelerations, multiplied by the respective arms, while the last term is the lateral component of the gravity acceleration originated by the roll angle. A more detailed description of the mathematical proof of equation (10) can be found in Perez (2006).

Ship passengers comfort evaluation has been discussed by various

authors, which propose proper parameters depending mainly on vertical accelerations mean value and frequency. The most used parameters are the Motion Sickness Incidence (MSI), proposed by O'Hanlon and McCauley (1973), and the Vomiting Incidence (VI), by Lawther and Griffin (1986, 1988). In this study, MSI has been used to estimate crew comfort. The MSI at point P for a reference exposition time of 2 h is given by the following equation (Cepowski, 2012; Piscopo and Scamardella, 2015), in dependence of the spectral moments of the absolute vertical motion η_{3P}:

$$MSI = 100\left[0.5 + \mathrm{erf}\left(\frac{\log_{10}\frac{a_v}{g} - \mu_{MSI}}{0.4}\right)\right] \tag{11}$$

where g is the gravitational acceleration, $\mathrm{erf}(x)$ is the error function, and a_v and μ_{MSI} are defined as follows:

$$\begin{aligned} a_v &= 0.798\sqrt{m_{4,\eta_{3P}}} \\ \mu_{MSI} &= -0.819 + 2.32\left[\log_{10}\sqrt{\frac{m_{4,\eta_{3P}}}{m_{2,\eta_{3P}}}}\right]^2 \end{aligned} \tag{12}$$

3.3. Propulsion

The propeller performance simulation is carried out by using the open water diagrams reporting thrust and torque coefficients, K_T and K_Q respectively, versus advance coefficient J respectively defined as follows:

$$J = \frac{V_a}{nD} \tag{13}$$

$$K_T = \frac{T}{\rho n^2 D^4} \tag{14}$$

$$K_Q = \frac{Q}{\rho n^2 D^5} \tag{15}$$

where ρ is the density of water, T and Q are the propeller open water thrust and torque, V_a is the propeller advance speed, n is the propeller revolution speed and D is the propeller diameter. The propeller revolutions are evaluated imposing the equilibrium between required vs delivered thrust by using the auxiliary variable $\frac{K_T}{J^2}$ is used. The engine power is computed in accordance to the following equation:

$$P_B = \frac{2\pi\rho_{H_2O} n^3 D^5 K_Q}{\eta_r \eta s \eta_g} \tag{16}$$

where η_r, ηs, η_g are the relative rotative efficiency, the shaft efficiency and the gearbox efficiency respectively considered as constant values. The engine fuel mass flow rate $\dot{m}_f$ is evaluated by using the engine performance map modelled using the engine MCR power and revolution. By the performance map each working conditions are checked for not exceeding the engine limits (Fig. 2). The feasibility or infeasibility of any combination of speed and weather conditions as well as the associated cost in terms of fuel consumption are thus a result of the propulsion simulation. The procedure is summarized in Algorithm 1.

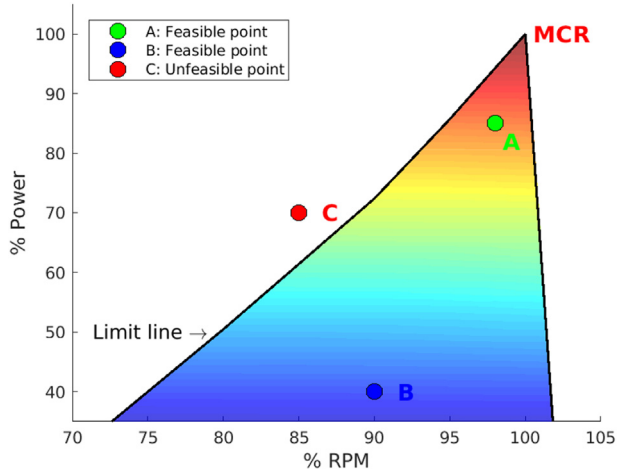

Fig. 2. Feasibility check of propulsion system working points.

Algorithm 1. Fuel mass flow rate computation procedure.

function FuelMassFlowRate($V_{ship}, \lambda, \varphi, t$)
  interpolate $R_t(V_{ship}$
  estimate weather at (λ, φ, t) from maps
  compute seakeeping indices
  if seakeeping constraints violated **then**
    return NaN
  else
    compute R_{tot} (eq. 3, 4, 5)
    compute required thrust T_r
    compute $\frac{K_{T_r}}{J^2}$
    interpolate J and K_Q
    compute N and P_B (eq 12,16)
    interpolate $\dot{m}_f$ in the engine map
    return $\dot{m}_f$

The mass of fuel burned m_f of each route segment is evaluated by numerical integration of the fuel mass flow rate with respect to time as shown in equation (17):

$$m_{f(X_i,t_i)\to(X_j,t_j)} = \int_{t_i}^{t_j} \dot{m}_f(t)dt \tag{17}$$

where is supposed to ship travel from point X_i at time t_i to point X_j at time t_j.

Expression 17 allows to compute the cost function at each DP step. The cost of the whole voyage is obtained by summation of all the contributes.

4. Route parametrization

A parametric definition of the ship voyage is needed in order to perform the optimization. The proposed parametrization is based on great circle geometry in order to easily identify the shortest solution: in an optimal solution any deviation from the great circle is thus caused by rough weather.

The minimum angular distance Θ_{AB}, measured in radiants, between two points A and B satisfies the following relationship:

$$\begin{aligned} \cos\Theta_{AB} &= \sin\varphi_A \sin\varphi_B + \\ &+ cos\varphi_A \cos\varphi_B \cos(\lambda_B - \lambda_A) \end{aligned} \tag{18}$$

where φ_A, φ_B, λ_A, λ_B, denote latitude and longitude of the points.

The course α is defined as the angle between the ship heading and the true north direction, it is measured clockwise and it changes continuously along a segment of great circle. The following relationships provide the initial and final course angles, respectively α_i and α_f, of the great circle segment linking points A and B:

$$\cos\alpha_i = \frac{\sin\varphi_B - \sin\varphi_A\cos\Theta_{AB}}{\cos\varphi_A\sin\Theta_{AB}} \tag{19}$$

$$\cos\alpha_f = \frac{\sin\varphi_B\cos\Theta_{AB} - \sin\varphi_A}{\cos\varphi_B\sin\Theta_{AB}} \tag{20}$$

The geographical coordinates of a point X laying on the great circle segment linking A and B and the local course angle are given by the following equations:

$$\sin\varphi_X = \sin\varphi_A + \cos(m_{AB}x) + \\ +\cos\varphi_A\sin(\Theta_{AB}x)\cos\alpha_i \tag{21}$$

$$\cos(\lambda_X - \lambda_A) = \frac{\cos(\Theta_{AB}x)}{\cos\varphi_A\cos\varphi_X} - \\ +\tan\varphi_A\tan\varphi_X \tag{22}$$

$$\cos\alpha_X = \frac{\sin\varphi_X\cos(\Theta_{AB}x) - \sin\varphi_A}{\cos\varphi_X\sin(\Theta_{AB}x)} \tag{23}$$

where $x = \frac{\Theta_{AX}}{\Theta_{AB}}$ is an advance parameter.

The coordinates of points Y are given as a function of the deviation parameter δ by the following expressions:

$$\varphi_Y = \varphi_X - \delta\sin\alpha_X \tag{24}$$

$$\lambda_Y = \lambda_X + \sigma\delta\cos\alpha_X \tag{25}$$

where $\sigma = 1$ going eastward and $\sigma = -1$ going westward. Fig. 3 summarizes the above presented sets of equations.

In the proposed dynamic programming framework the ship route is modelled as a finite set of way points $\{X_0, X_1, \ldots, X_n\}$ such that $X_i = (\lambda_i, \varphi_i)$ and a corresponding set of arrival times at the way points, $\{t_0, t_1, \ldots, t_n\}$, where $t_0 = 0$ and $t_n = ETA$. Each segment $X_i \rightarrow X_{i+1}$, is sailed at constant speed V_i.

The described scheme allows to identify unequivocally the great circle i.e. minimum distance solution which is the most convenient in calm sea and obstacle-free conditions.

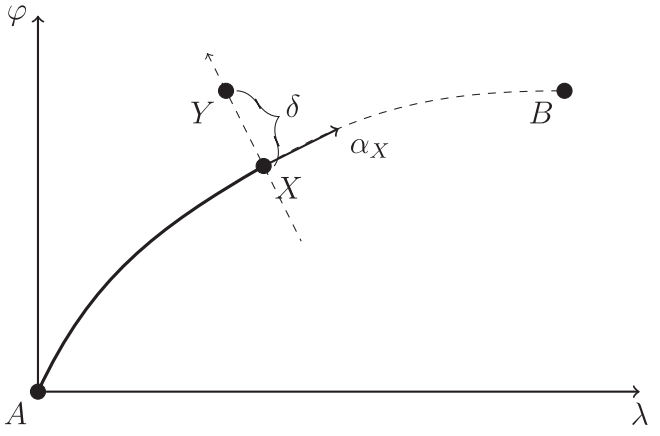

Fig. 3. Deviation δ of point Y from the corresponding point X laying on great circle segment linking A and B.

5. Dynamic programming optimization

Dynamic programming is an optimization strategy that aims to solve a problem by using a multi-stage approach in which the final result is the consequence of a number of separate decisions. Optimal solution is found on the basis of Bellmans principle of optimality:

> "an optimal policy has the property that whatever the initial state and initial decision are, the remaining decisions must constitute an optimal policy with regard to the state resulting from the first decision" (Bellman, 1954).

The structure of the method well adapts to any multi stage decision process and among all 'best path search' type problems (Bellman, 1958), (Bellman, 1962), as they can be reduced as a sequence of decisions in dependance of which a return is obtained.

5.1. Formalization

The proposed formulation of the ship voyage optimization problem is solved in a three dimensional domain: start and arrival points and time instants are assigned a-priori, then a two dimensional domain is identified by discretizing parameters x and δ in equations (21)–(25) (Fig. 4). A discretization of the time axis (Fig. 5) is as well performed. The route is modelled as finite set of N+1 way points through which the ship passes at assigned times. The ship is supposed to travel at constant speed between each pair of waypoints. The route r is thus given by the following sets:

$$r : \begin{cases} X &= \{X_0, X_1, \ldots, X_N\} \\ t &= \{t_0, t_1, \ldots, t_N\} \end{cases} \tag{26}$$

where $X_i = (\lambda_i, \varphi_i)$, $X_0 = A$, $X_N = B$, $t_0 = 0$, $t_N = ETA$.

Equation (17) allows to compute the fuel $m_{f\ (X_i,t_i)\rightarrow(X_j,t_j)}$ consumed from point X_i at time t_i to point X_j at time t_j steaming at constant speed.

The objective of the problem is to minimize the total fuel consumption:

$$m_f = \sum_{i=0}^{N-1} m_{f\ (X_i,t_i)\rightarrow(X_{i+1},t_{i+1})} \tag{27}$$

The problem can be written in the form of the Bellman's equation as follows. Let $f_i(X,t)$ be the fuel consumed at stage i from the start, following an optimal policy, being the ship in position X at time t: the target of the search is thus $f_N(X_N, ETA)$, i.e. the mass of fuel consumed at the end of the voyage identified by the arrival point X_N and estimated time of arrival ETA, following an optimal policy. In accordance to Bellman's Principle of Optimality, the following functional relationship can be written:

$$f_i(X,t) = \min_{\xi,\tau}\left[m_{f(\xi,\tau)\rightarrow(X,t)} + f_{i-1}(\xi,\tau)\right] \tag{28}$$

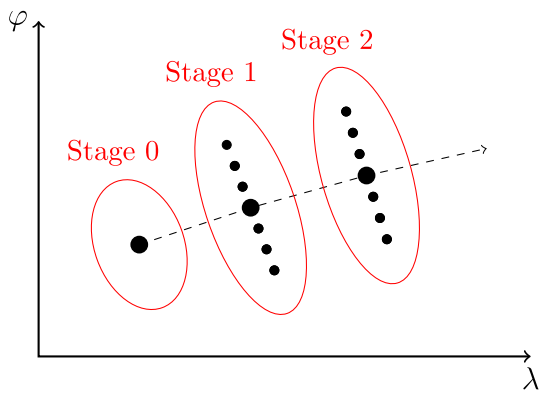

Fig. 4. A schematic representation of the geographical search grid.

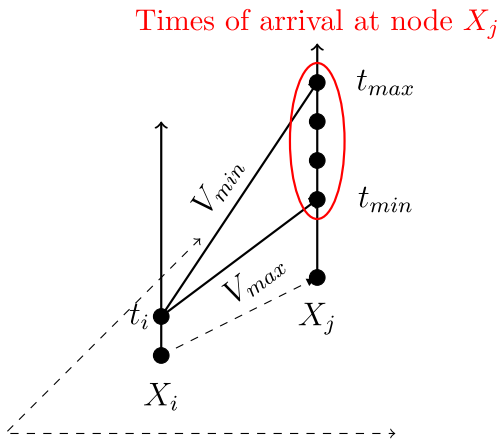

Fig. 5. A representation of the times of arrival at each grid node.

where ξ and τ represent the possible positions and times of arrival at stage $i-1$.

5.2. Computational aspects

DP is an exhaustive approach, i.e. it guarantees to identify the optimal solution associated to the discretization of the problem. Nevertheless, this advantage over heuristic global search algorithms is partially limited by the fact that input data is affected by significant uncertainties. DP presents some drawbacks in terms of compuatation speed: Bellman-Ford implementation on a graph (Bellman, 1958) runs in $O(|V||E|)$, where $|V|$ and $|E|$ are the number of graph and edges respectively. In the present work, the breadth-first-search structure of the Bellman-Ford algorithm has been maintained, however a significant speed-up has been made by implementing problem-specific modifications to the algorithm.

In the proposed solution scheme the cost of each route segment linking each couple of nodes (all geographical positions and all time instants) is evaluated in the forward phase. The search domain is progressively explored following a breadth-first approach. Nodes are sorted by priority to minimize the number of segments estimations: a computationally cheap lower bound of the cost of each segment is first computed in order to early prune the less promising solutions. The compliance of each node with the time of arrival window is checked as early as possible. Nodes visibility based on geographical constraints is checked by using an efficient nearest neighbour search algorithm based on kd-tree structures (Friedman et al., 1977) before evaluating the cost of each segment. The cost associated to each segment is computed by numerical integration of the ship model output.

At the end of the calculation a number of nodes, characterized by a time of arrival (i.e the ETA), and a cost associated (fuel consumption) are identified. The final nodes identify global optima in terms of fuel consumption at fixed time or the fastest solutions at fixed fuel consumption. The final set of nodes can thus be seen as the Pareto Frontier of a two objective optimization problem which aims to minimize both time of arrival and fuel consumption. Each node contains the information of the previous one, so each solution is extracted by back-tracking.

The optimization routine has been developed and implemented by the authors in C++ language, significantly relying on C++ Standard Template Library. Armadillo linear algebra library (Sanderson, 2010) has been used for basic matrix manipulation.

6. Case study

The above described optimization code has been tested on a bulk carrier to evaluate the effectiveness of the adopted optimization strategy. The main data of the considered vessel are summarized in Table 1. The still water resistance has been calculated in accordance with the method proposed by Holtrop (1984). Wind resistance coefficient c_X has been computed according to the method proposed by Blendermann (1994). Finally, open source strip theory seakeeping code PDSTRIP (Bertram et. al, 2006) has been used to evaluate the pseudo response amplitude operator Φ_{aw} and ship motions absolute RAOs. The optimization is performed with reference to a voyage representing a North Atlantic crossing.

6.1. Grid setup

Two optimization modes are compared: a speed profile optimization, in which no deviations from the great circle route are allowed (referred as speed optimization, SO), and a speed and course optimization (referred as voyage optimization, VO) in which both speed and course adjustments are performed in order to achieve the optimum. Moreover, a constant speed great circle solution is presented for comparison.

A 10 stages by 11 steps grid with $\pm 1^\circ$ maximum deviation is considered: the resulting waypoints are about 300 miles apart. Times of arrival are discretized every 60 min, while integration time step is set to 30 min. The computation is carried out considering a time of arrival window between 200 and 400 h from departure.

6.2. Constraints

Ship safety and comfort constraints are imposed as well, in particular, slamming and deck wetness probabilities are checked (Journée, 1976; Journée and Meijers, 1980) in accordance with the following inequalities:

$$P\left(\eta_{3r,0.9L} > T, \dot{\eta}_{3r,0.9L} > 0.093\sqrt{gL}\right) < 0.03 \tag{29}$$

$$P\left(\eta_{3r,B} > f_b\right) < 0.07 \tag{30}$$

$$P\left(\ddot{\eta}_{3,B} > 0.4g\right) < 0.07 \tag{31}$$

Being $\eta_{3r,0.9L}$ and $\eta_{3r,B}$ the relative vertical motion at 90% of the ship length and at bow respectively, L, T and f_b the ship length, draft and free board at the bow respectively.

In addition, the following inequality constraints are imposed:

$$LFE_{RMS} < LFE_{max} \tag{32}$$

$$MSI < MSI_{max} \tag{33}$$

Where MSI_{max} has been set to 10%, LFE_{RMS} is the root mean square of the lateral force estimator, and LFE_{max} has been selected in accordance with (Perez, 2006), who proposes $0.1g$ as an upper bound for general purposes.

6.3. Weather forecasts

The forecasts used for the test case are based on the National Weather Service (NOAA) Wave Watch III model which provides forecast maps every 6 h. The files are available in GRIB format, they are 162 h deep, they have a $1.25^\circ \times 1^\circ$. grid resolution and a 6 h time resolution (NOAA MMAB Operational Wave Model). The weather forecasts have been downloaded from: http://www.globalmarinenet.com.

Table 1
Main characteristics of the case study ship.

Ship type	Bulk Carrier
Length b. p.	182 m
Beam	31 m
Draft	9 m
Displacement	41577 t
Propeller	1 × FPP, 4 blades, Diameter = 6 m
Main engine	1 × 10 MW, 113 RPM 2 stroke diesel engine

In particular, the case study optimization is carried out in a typical Northern Atlantic winter rough weather condition, using the forecast maps of day 2016/01/21, 12:00 a.m. An example screenshot of the storm occurring is shown in Fig. 6.

6.4. Results

Fig. 7 shows the fuel consumption vs. ETA trade off curve. Each point of the curve is the minimum fuel consumption solution at the corresponding ETA, i.e. the curve can be seen as the Pareto Frontier of the minimum ETA and minimum fuel consumption optimization problem. VO and SO solutions are compared and the results achievable by sailing at constant speed are reported for comparison. Note that the course and speed optimization curve (VO) has a significant lower consumption with respect to the other two, however also speed optimization (SO) provides good results especially for high ETAs.

Note in addition that both the optimization strategies allow to reduce the negative effect of involuntary speed reduction on the ETA, allowing thus to achieve lower times of arrival by adjusting speed and course to the weather conditions, i.e. catching up the lost time when the weather conditions are better. Moreover, each of the suggested solutions is the most fuel saving strategy to perform the voyage in the assigned time. Finally, note that Fig. 7 allows to easily estimate the cost of each hour of anticipation or delay in terms of tons of fuel consumed.

The trajectories associated to different ETAs (220, 250 and 300 h) are presented in Figs. 8–10. The corresponding speed profiles are presented in Figs. 11–13. It is worth noting that the optimization algorithm VO acts drastically on ship speed to search the optimum, finding articulated speed profiles.

The route and/or speed adjustments allow a global reduction of the fuel mass flow rate required by the propulsion system (Figs. 14–16) resulting in a reduction of the total energy requirement and CO2 emissions. The fuel consumption profiles are presented in Figs. 17–19.

The solutions presented until now are referred to a westward voyage: this direction is associated to head or bow sea mainly. If the opposite voyage in the same day of departure is considered, the solutions change radically: the fuel consumption to ETA curves of the two voyages are compared in Fig. 20. The eastward voyage presents significantly lower fuel consumption as expected: the following sea condition is predominant, thus the added resistance is lower. Moreover, lower ETAs are achievable as the weather conditions are less severe: involuntary speed reduction is thus less significant. In addition, the eastward optimized solutions do not present significant fuel saving with respect to the constant speed solution, if compared to the westward ones due to the fact that the course and speed changes have small effect on the hydrodynamic resistance in following seas. Fig. 21 presents the trajectories in the two cases, associated to an ETA of 250 h: note that the suggested routes are significantly different, due to the different the conditions encountered.

Note finally that sailing in following sea may lead to significant lateral motions. The constraint on lateral forces allows to limit these effects, however a check of parametric roll (Maki et al., 2011) might be included in a future version.

6.5. Computational time

The above presented computations have been carried out on a standard laptop which main data are summarized in Table 2. The computation time is significantly influenced by the chosen discretization parameters and by the set up of the constraints. The average computation times achieved are presented in Table 3. The computation times required in case a unique ETA with no delay is selected are also reported: note that the computation in this case is significantly faster. On the contrary the computation time increases as the ETA window gets wider. In general, the more the problem is constrained, the less nodes are processed, resulting in a faster computation.

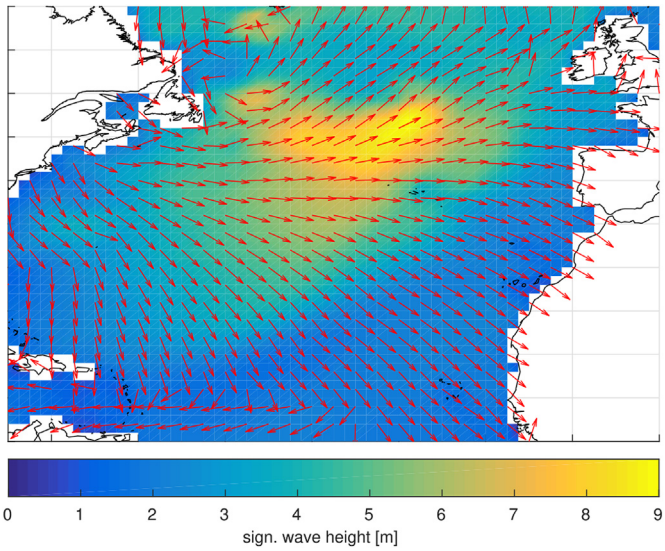

Fig. 6. An example map of the weather forecast used as a case study.

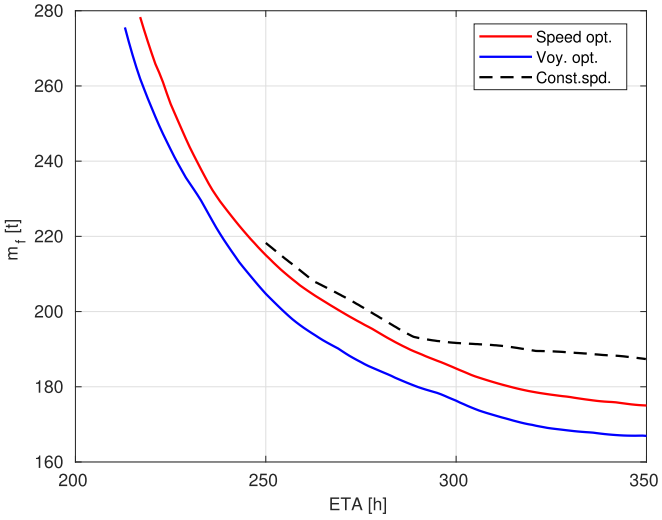

Fig. 7. Fuel consumption to ETA trade off for the considered case study voyage.

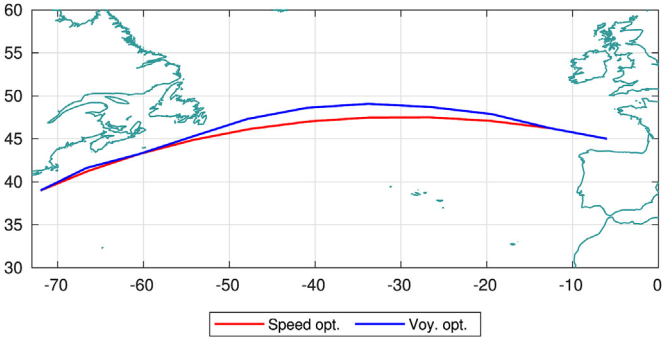

Fig. 8. Optimal routes for ETA = 220 h.

7. Conclusions

A ship voyage optimization method has been developed and presented, aiming to find the minimum fuel consumption voyage, subject to

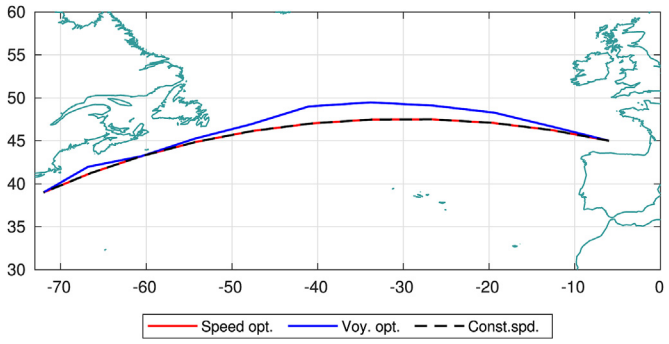

Fig. 9. Optimal routes for ETA = 250 h.

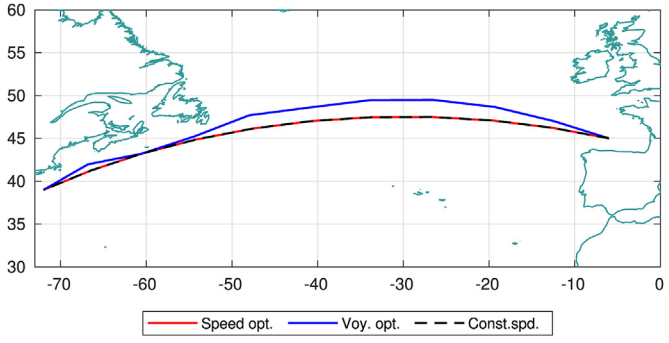

Fig. 10. Optimal routes for ETA = 300 h.

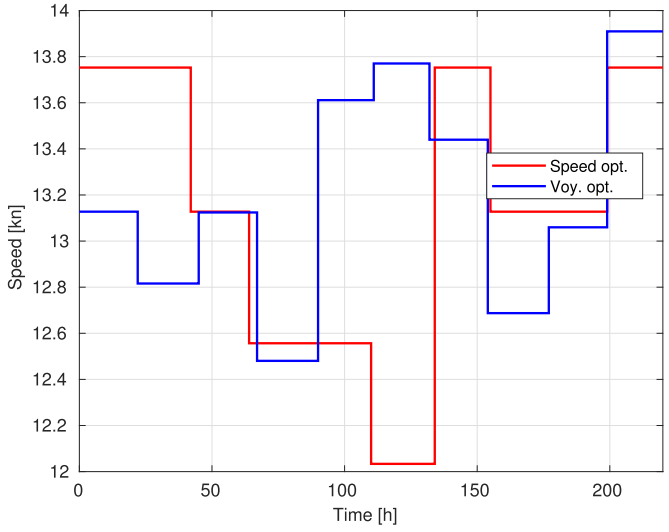

Fig. 11. Optimal speed profiles for ETA = 220 h.

safety and comfort constraints, by using 3D Dynamic Programming optimization. A steady state ship model has been described. The model computes the seakeeping and propulsion performances of the ship in assigned wind and wave conditions. A parametric route model, based on great circle navigation, has been introduced, in order to give a dynamic programming formulation of the problem. The solution is found by solving the Bellman's equation which cost function, i.e. the total mass of burned fuel, is evaluated by means of a ship steady sate simulation model. In order to take into account ship safety and crew comfort in the optimization, slamming, deck wetness and high bow acceleration probabilities, as well as motion sickness incidence and lateral forces in the crew accommodations are checked not to exceed threshold values. An

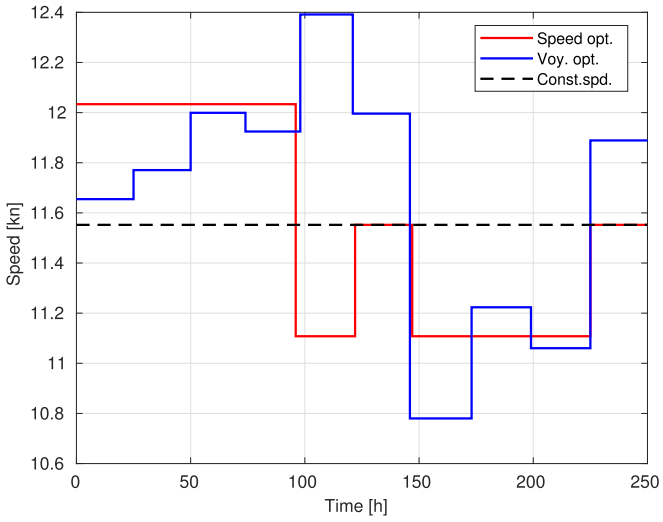

Fig. 12. Optimal speed profiles for ETA = 250 h.

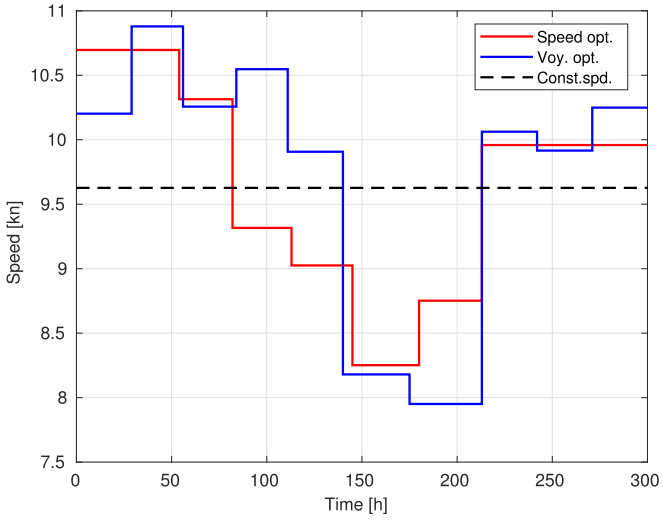

Fig. 13. Optimal speed profiles for ETA = 300 h.

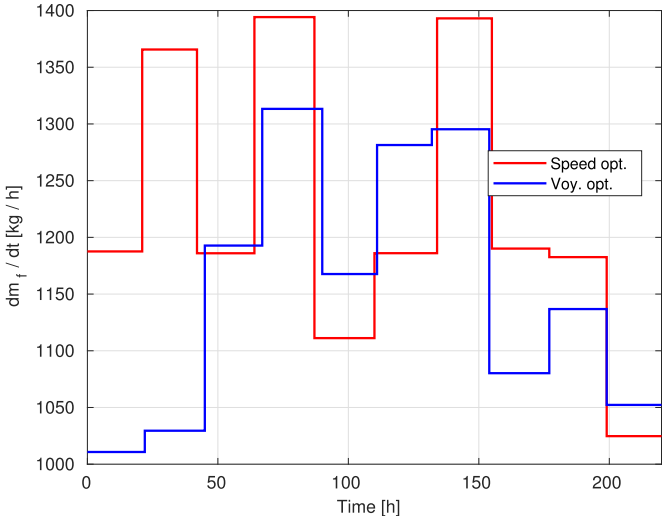

Fig. 14. Fuel mass flow rate profiles for ETA = 220 h.

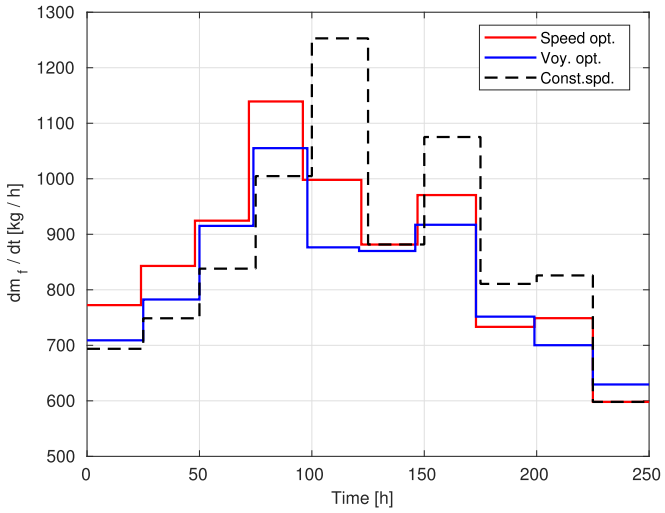

Fig. 15. Fuel mass flow rate profiles for ETA = 250 h.

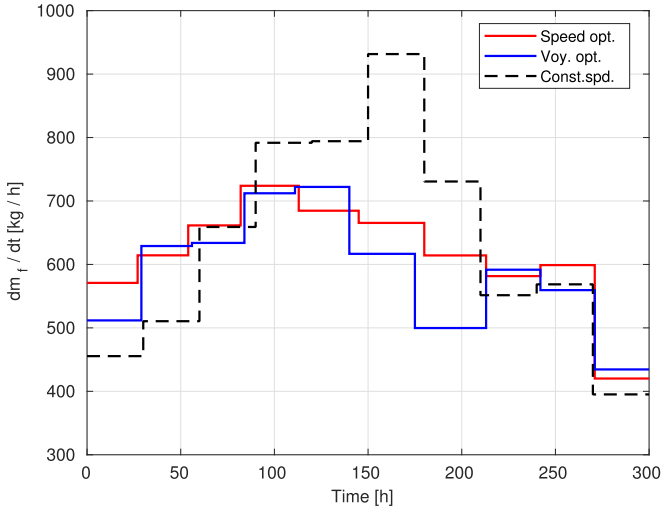

Fig. 16. Fuel mass flow rate profiles for ETA = 300 h.

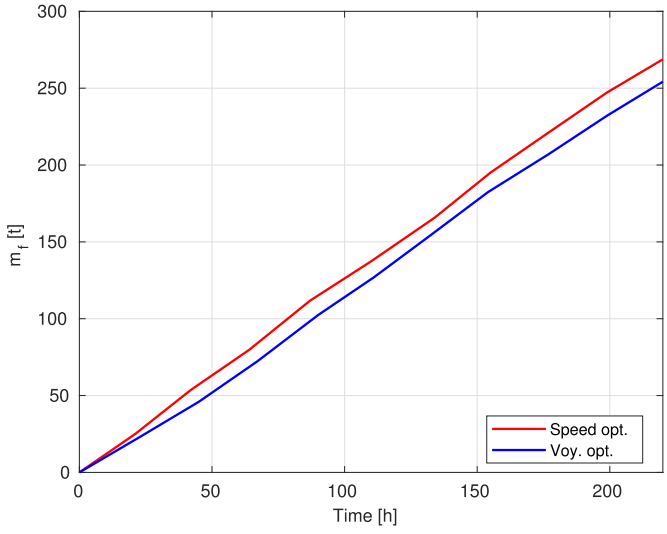

Fig. 17. Fuel consumption profiles for ETA = 220 h.

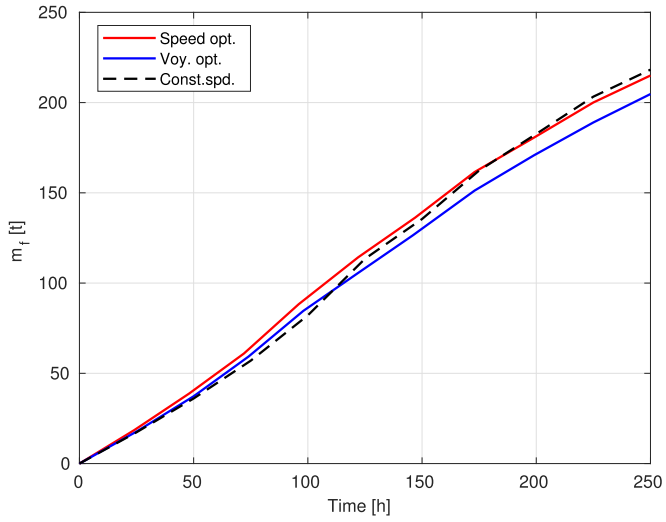

Fig. 18. Fuel consumption profiles for ETA = 250 h.

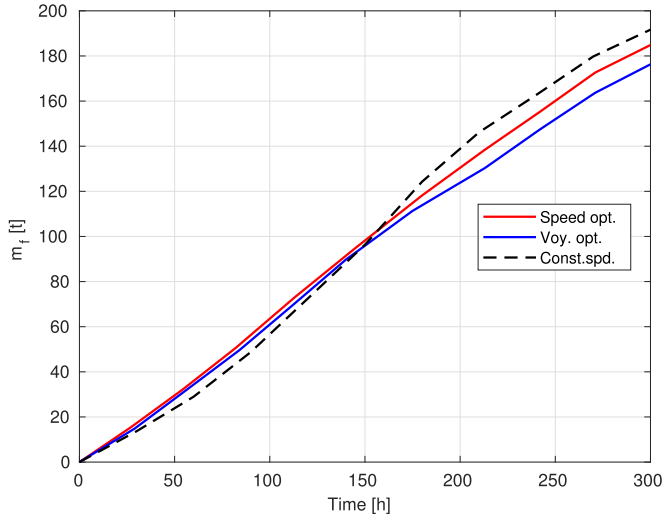

Fig. 19. Fuel consumption profiles for ETA = 300 h.

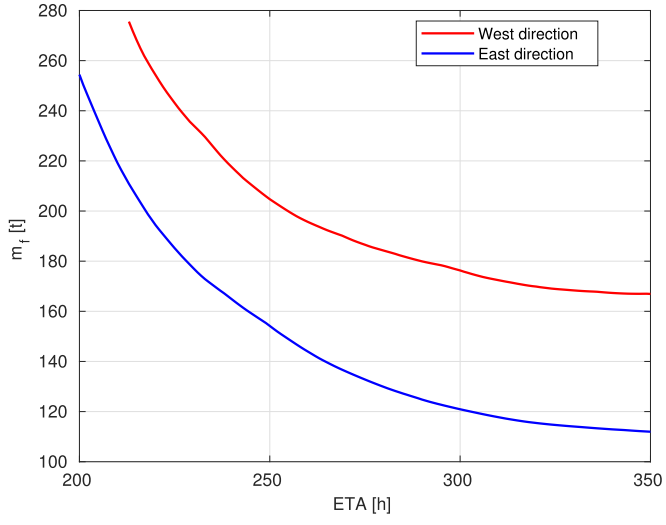

Fig. 20. Fuel consumption to ETA trade off of eastward vs. westward voyages.

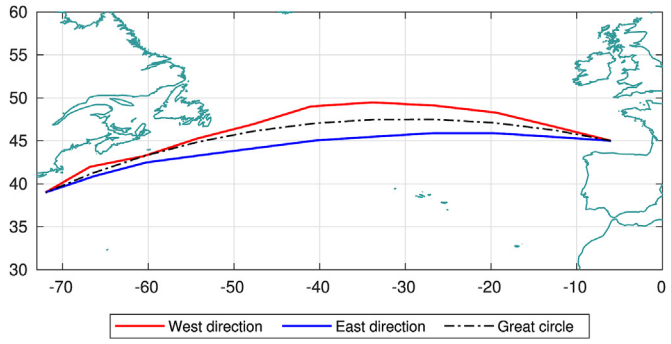

Fig. 21. Trajectories of eastward vs. westward voyages for ETA = 250 h.

Table 2
Main data of the PC used for computation.

Processor	Intel Core i7-6500U
Memory	16 GB
OS	Ubuntu 16.04 64-bit
C/C++ Compiler	GCC

Table 3
Time required by computations.

Computation	Time	Num. sol.
Speed opt. (no delay)	<1″	1
Voy. opt. (no delay)	1′ 20″	1
Speed opt. (Pareto)	6″	134
Voy. opt. (Pareto)	10′ 50″	134

algorithm has been developed and implemented by the authors in C++ language to solve the proposed task. The presented approach has been applied to a case study voyage from France to New York along the Atlantic Ocean: the results associated to a constant speed voyage, a speed profile only optimization, and a full speed and course optimization have been compared: the presented results include the voyage time to fuel consumption trade-off curves, the optimal trajectories and speed profiles obtained for different voyage times. Moreover, fuel mass flow rate and fuel consumption profiles associated to the considered solutions have been discussed. The sensitivity of the optimization procedure to different weather conditions has been tested by optimizing the reverse voyage in the same days. In light of the obtained results a notable fuel saving potential is observed, in particular in the voyage optimization (VO) case, in which the algorithm takes full advantage from the ship propulsion model features.

References

Altosole, M., Benvenuto, G., Campora, U., Laviola, M., Zaccone, R., 2017. Simulation and performance comparison between diesel and natural gas engines for marine applications. Proc. Inst. Mech. Eng. M J. Eng. Marit. Environ. 231 (2), 690–704.

Altosole, M., Benvenuto, G., Figari, M., Campora, U., Bagnasco, A., D'Arco, S., Giuliano, M., Giuffra, V., Spadoni, A., Zanichelli, A., Michetti, S., Ratto, M., 2008. Real time simulation of the propulsion plant dynamic behaviour of the aircraft carrier "cavour". In: Proceedings of the Institute of Marine Engineering, Science and Technology - INEC 2008: Embracing the Future.

Altosole, M., Figari, M., Ferrero, C., Giuffra, V., Piva, L., 2014. Propulsion retrofitting of the tall ship amerigo vespucci: automation design by simulation. In: 2014 International Symposium on Power Electronics, Electrical Drives, Automation and Motion, SPEEDAM 2014, pp. 313–318.

Altosole, M., Piastra, F., Canepa, E., 2016. Performance analysis of a motor-sailing propulsion system for control design purposes. Ships Offshore Struct. 11 (7), 688–699.

Bellman, R., 1954. The Theory of Dynamic Programming, Technical Report, DTIC Document.

Bellman, R., 1958. On a routing problem. Q. Appl. Math. 87–90.

Bellman, R., 1962. Dynamic programming treatment of the travelling salesman problem. J. ACM 9 (1), 61–63.

Bertram, V., Veelo, B, Soding, H., 2006. Program PDSTRIP: Public Domain Strip Method. Hamburg, unpublished.

Blendermann, W., 1994. Parameter identification of wind loads on ships. J. Wind Eng. Ind. Aerod. 51 (3), 339–351.

Cepowski, T., 2012. The Prediction of the Motion Sickness Incidence Index at the Initial Design Stage. Zeszyty Naukowe/Akademia Morska w Szczecinie, pp. 45–48.

Chen, H., 2013. Voyage optimization supersedes weather routing. Jeppesen Commerc. Mar. J.

Coraddu, A., Figari, M., Savio, S., Villa, D., Orlandi, A., 2013. Integration of seakeeping and powering computational techniques with meteo-marine forecasting data for in-service ship energy assessment. In: Developments in Maritime Transportation and Exploitation of Sea Resources: IMAM 2013, p. 93.

Fang, M.C., Lin, Y.H., 2015. The optimization of ship weather-routing algorithm based on the composite influence of multi-dynamic elements (ii): optimized routings. Appl. Ocean Res. 50, 130–140.

Friedman, J.H., Bentley, J.L., Finkel, R.A., 1977. An algorithm for finding best matches in logarithmic expected time. ACM Trans. Math Software (TOMS) 3 (3), 209–226.

Holtrop, J., 1984. Statistical re-analysis of resistance and propulsion data. Int. Shipbuild. Prog. 31 (363), 272–276.

ISO 2631-1: 1997, 1997. Mechanical Vibration and Shock: Evaluation of Human Exposure to Whole-body Vibration. Part 1, General Requirements: International Standard ISO 2631-1: 1997 (E). ISO.

James, R.W., 1957. Application of Wave Forecasts to Marine Navigation.

Journée, J.M.J., 1976. Prediction of Speed and Behaviour of a Ship in a Sea-way. Delft University of Technology.

Journée, J.M.J., Meijers, J.H.C., 1980. Ship Routeing for Optimum Performance. Delft University of Technology.

Lawther, A., Griffin, M.J., 1986. The motion of a ship at sea and the consequent motion sickness amongst passengers. Ergonomics 29 (4), 535–552.

Lawther, A., Griffin, M.J., 1988. A survey of the occurrence of motion sickness amongst passengers at sea. Aviat Space Environ. Med. 59 (5), 399–406.

Lewis, E.V., 1989. Principles of Naval Architecture. second revision. In: Motions in Waves and Controllability, iii. The Society of Naval Architects and Marine Engineers, Jersey City, USA.

Lin, Y.H., Fang, M.C., Yeung, R.W., 2013. The optimization of ship weather-routing algorithm based on the composite influence of multi-dynamic elements. Appl. Ocean Res. 43, 184–194.

Lu, R., Turan, O., Boulougouris, E., Banks, C., Incecik, A., 2015. A semi-empirical ship operational performance prediction model for voyage optimization towards energy efficient shipping. Ocean Eng. 110, 18–28.

Maki, A., Akimoto, Y., Nagata, Y., Kobayashi, S., Kobayashi, E., Shiotani, S., Ohsawa, T., Umeda, N., 2011. A new weather-routing system that accounts for ship stability based on a real-coded genetic algorithm. J. Mar. Sci. Technol. 16 (3), 311–322.

Marie, S., Courteille, E., et al., 2009. Multi-objective optimization of motor vessel route. Mar. Navig. Saf. Sea Transport. 411.

Martelli, M., Figari, M., Altosole, M., Vignolo, S., 2014a. Controllable pitch propeller actuating mechanism, modelling and simulation. Proc. Inst. Mech. Eng. M J. Eng. Marit. Environ. 228 (1), 29–43.

Martelli, M., Viviani, M., Altosole, M., Figari, M., Vignolo, S., 2014b. Numerical modelling of propulsion, control and ship motions in 6 degrees of freedom. Proc. Inst. Mech. Eng. M J. Eng. Marit. Environ. 228 (4), 373–397.

Mentaschi, L., Besio, G., Cassola, F., Mazzino, A., 2015. Performance evaluation of wavewatch iii in the mediterranean sea. Ocean Model. 90, 82–94.

O'Hanlon, J.F., McCauley, M.E., 1973. Motion Sickness Incidence as a Function of the Frequency and Acceleration of Vertical Sinusoidal Motion, Technical Report, DTIC Document.

Papadakis, N.A., Perakis, A.N., 1990. Deterministic minimal time vessel routing. Oper. Res. 38 (3), 426–438.

Perez, T., 2006. Ship Motion Control: Course Keeping and Roll Stabilisation Using Rudder and Fins. Springer Science & Business Media.

Piscopo, V., Scamardella, A., 2015. The overall motion sickness incidence applied to catamarans. Int. J. Naval Architect. Ocean Eng. 7 (4), 655–669.

Safaei, A., Ghassemi, H., Ghiasi, M., 2015. Voyage Optimization for a Very Large Crude Carrier Oil Tanker: a Regional Voyage Case Study. Zeszyty Naukowe/Akademia Morska w Szczecinie.

Sanderson, C., 2010. Armadillo: an Open Source C++ Linear Algebra Library for Fast Prototyping and Computationally Intensive Experiments.

Shao, W., Zhou, P., Thong, S.K., 2012. Development of a novel forward dynamic programming method for weather routing. J. Mar. Sci. Technol. 17 (2), 239–251.

Spentza, E., Besio, G., Mazzino, A., Gaggero, T., Villa, D., 2017. A ship weather-routing tool for route evaluation and selection: influence of the wave spectrum. In: Proceedings of the 17th International Congress of the International Maritime Association of the Mediterranean, IMAM 2017.

Vettor, R., Guedes Soares, C., 2016. Development of a ship weather routing system. Ocean Eng. 123, 1–14.

Zaccone, R., Figari, M., Altosole, M., Ottaviani, E., 2016. Fuel saving-oriented 3D dynamic programming for weather routing applications. In: Proceedings of the 3rd International Conference on Maritime Technology and Engineering, MARTECH 2016, p. 183189.

Zoppoli, R., 1972. Minimum-time routing as an n-stage decision process. J. Appl. Meteorol. 11 (3), 429–435.